

# RESONANCE FREQUENCY SHIFT EFFECTS DUE TO CAVITY LENGTH AND WINDOW VARIATION

G. Arriaga, Northern Illinois University, DeKalb, IL 60115, United States

K. Yonehara, Fermi National Laboratory, Batavia, IL, United States

## **Abstract**

Various kinds of Lepton colliders have been proposed for the energy frontier machine after discovering Higgs boson at LHC. Muon colliders seem to be the most efficient due to size and low synchrotron radiation compared to proposed electron-positron colliders. There has been a significant amount of analytical research, experimental efforts, and development in Radio Frequency (RF) cavities to accelerate muons, in their short lifetime, with the ultimate goal of building a muon collider. This paper focuses on how varying length of the RF cavities and bowing in cavity windows influence the resonance frequency and the electric field distribution.

## **Introduction**

Muons are viewed as good candidates for a lepton, or subatomic particle, collider as muon colliders would be more compact than most other colliders at the same center of mass. [1] The Muon collider design group meets several challenges. One issue is the current density of muon beams. Since muons are produced as tertiary particles, the size of a muon beam tends to be large. As a result, the luminosity in a collider is too small to discover unknown heavy particles. In order to increase the luminosity, Muon beams are concentrated with ionization cooling. The ionization cooling channel consists of a strong magnet and high gradient Radio Frequency (RF) cavity to reduce the size of the beam. [2] A present issue to make a cooling channel is that the resonant frequency in the RF cavity is shifted by distortion of the RF cavity window, which is the entrance of the muon beam. The distortion is caused by Lorentz force detuning and thermal expansion. It is important to know what amount of a dynamic range of resonant frequency shift is, namely how much the incident muons gain accelerating energy, from the RF cavity in the cooling channel. Research efforts in this paper focus on simulated RF cavity window distortion and resulting impact such distortions have on the resonance frequency and electric field inside a RF cavity.

## Methods and experiment

All test cavity simulations were run on the program SuperFish (SF), which is a program that can calculate static magnetic and electric fields as well as radio-frequency electromagnetic fields [3]. SF works by having the user input or type code and values for the cavity dimensions, material properties, starting frequency, ect into a file called automesh (figure 1). Values inputted into automesh are used by SF to solve desired RF cavity problems, such as frequency shift under various conditions. SF simplifies the RF geometry by using the boundary condition. Since the cavity of our interests has axial-symmetry, SF can estimate the EM field in half of the RF cavity. Therefore, a simple rectangular shape was efficient to use in SF.

```

Windowstudy_H_01-03 - Notepad
File Edit Format View Help
Windowstudy_H_0.1-0.3, f0 = 650.60 MHz

; Copyright 1998, by the University of California.
; Unauthorized commercial use is prohibited.

&reg kprob=1,          ; Superfish problem
icylin=1,            ; cylindrical symmetry
dx=0.2,              ; X mesh spacing
dy=0.2,
freq=650.0,          ; Starting frequency in MHz
xdri=2.0, ydri=17.65 ; Drive point location

&po x=2.0, y=17.65 &
&po x=2.0, y=2.0 &
&po nt=5, radius=6.8166667, x=2.3, y=0.0 &
&po x=22.3, y=0.0 &
&po nt=4, radius=6.8166667, x=22.0, y=2.0 &
&po x=22, y=17.65 &
&po x=2, y=17.65 &
    
```

Figure 1: example of an automesh input file.

Simulated cavities were assumed to be ideal and made of copper, at 1 atm filled with air. The original structure, or control structure, was a simple pillbox (figure 3). The design of the simple pillbox structure was gradually changed with curved or indented regions to simulate window bowing.

The radius of the test cavity was 17.65 cm, which is the result of calculations when the initial frequency is assumed to be 650 MHz, with window radii at a range of 2, 4, 8, 12, and 16 cm. The bow height of the windows ranged from 0.0 to 1 cm. There were three different cavity lengths simulated with the same

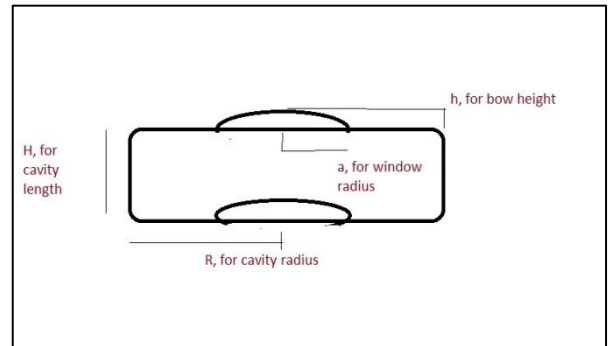


Figure 2: Sketch of cavity with bowed window concept.

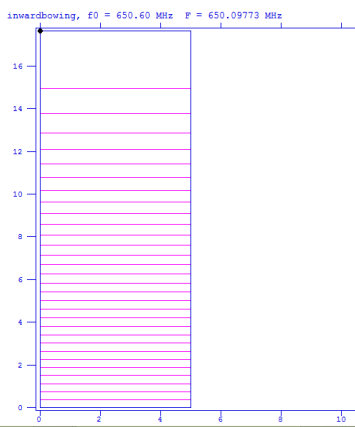


Figure 3: SF output image of a simple pillbox cavity with no bowing in cavity windows.

window distortion conditions. The lengths of the simulated cavities tested were 5 cm, 10 cm, a 20 cm (see figure 2). These conditions were inputted into automesh and run, or solved, by SF.

SF outputs provided information on the change in resonance frequency under each of the described conditions. The resulting frequencies obtained from superfish were plotted in Mathematica

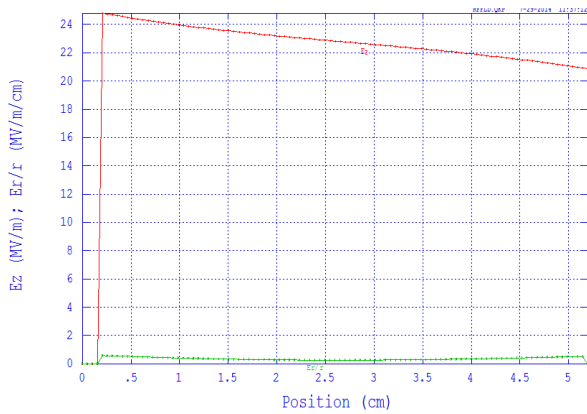


Figure 4: Parmela output displaying the electricfield in a cavity with window radius of 4 cm and bow height of 0.2 cm.

and fitted to observe the frequency shift trends as the cavity parameters were changed.

The SF outputs were further processed using a subprogram called Parmela, which solves for and displays electrostatic and magnetostatic problems, to show the change in the electric field between the two windows inside the simulated cavity (figure 4)

## Results and discussion

### Frequency change

Throughout each simulation, when windows were bowed in the same direction, SF outputs showed a similar trend. RF decreased as cavity window bow height increased. This trend was the same for each cavity length. When the data was plotted, the

trend of decrease seemed to follow a parabolic shape (see figure 5). Due to this observation a mathematical equation was proposed to model the trend and potentially predict the frequency change at any bow height. The equation proposed was  $f = f(1 + \alpha h^2)$ , where  $f$  is the change in frequency,  $\alpha$  is a constant that is a function of the cavity length and window radius, and  $h$  is

the height of the bow.

The data of frequency vs. the height of the bow was plotted for each cavity radius (figure 6). The graph showed a decrease in curvature as the window radius changed from 2 to 8 cm. However, there was an increase in curvature from 8 to 16 cm. From this observation, a 3x3 matrix was set up, using the 8 cm radius as a point of

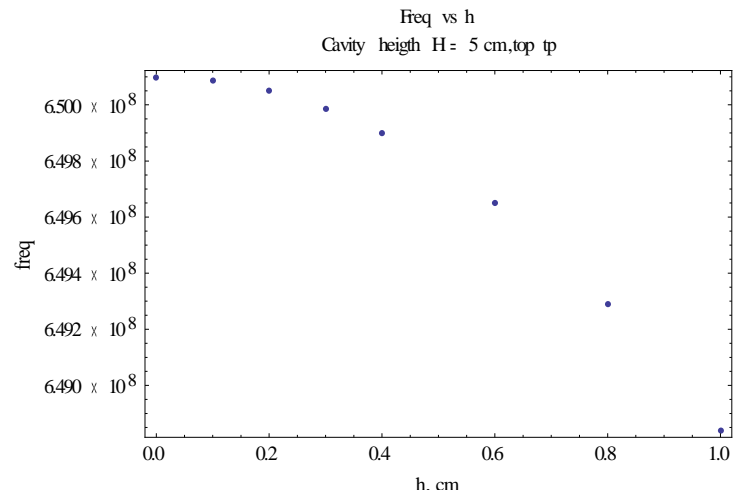


Figure 5: Plot of the change in resonance frequency vs. the height of the window bow for cavity with length 5 cm and window radius of 4 cm.

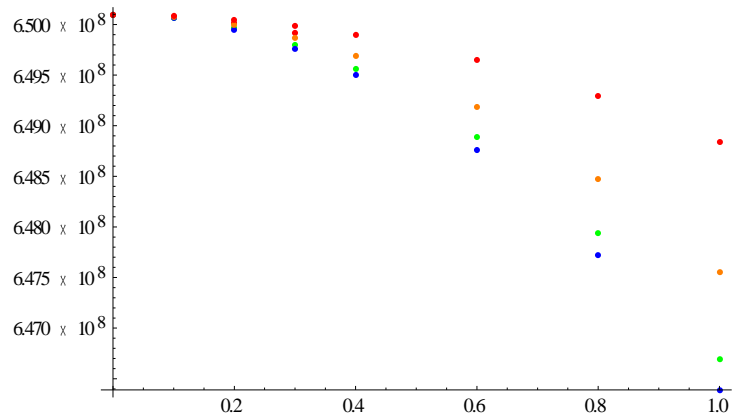


Figure 6: Plot of frequency vs. height of window bow for window radius 2(red), 4 (green), 8 (blue), and 12(orange) cm.

symmetry. The resulting scalar value was approximately  $3.423\text{cm}^{-2}$ . The standard deviation in the calculated constant was determined to be approximately  $\pm 382.128\text{cm}^{-2}$ .

Tests with windows bowing inward (figure 7) had a similar pattern to the data for the structure in which the windows were bowed in the same direction. The frequency decreased as the height of the bow increased. However, the minimum point occurred at a window radius of 12 cm.

Simulations with windows bowing outward (figure 7) had an inverse pattern compared to the data from the cavities with inward bowing windows.

### Electric Field

Analysis of the electric field, using the SF parameca table plot, revealed that the field decreases between the windows. The rate of decrease is significantly larger when the bow in the cavity window is larger (Figures 8).

The same pattern was seen in cavities with a larger window Radius. However, the phenomenon is greatly reduced (figure 8). The decrease in potential may indicate that the charged particles, muons in this case, are being accelerated as they pass through the cavity.

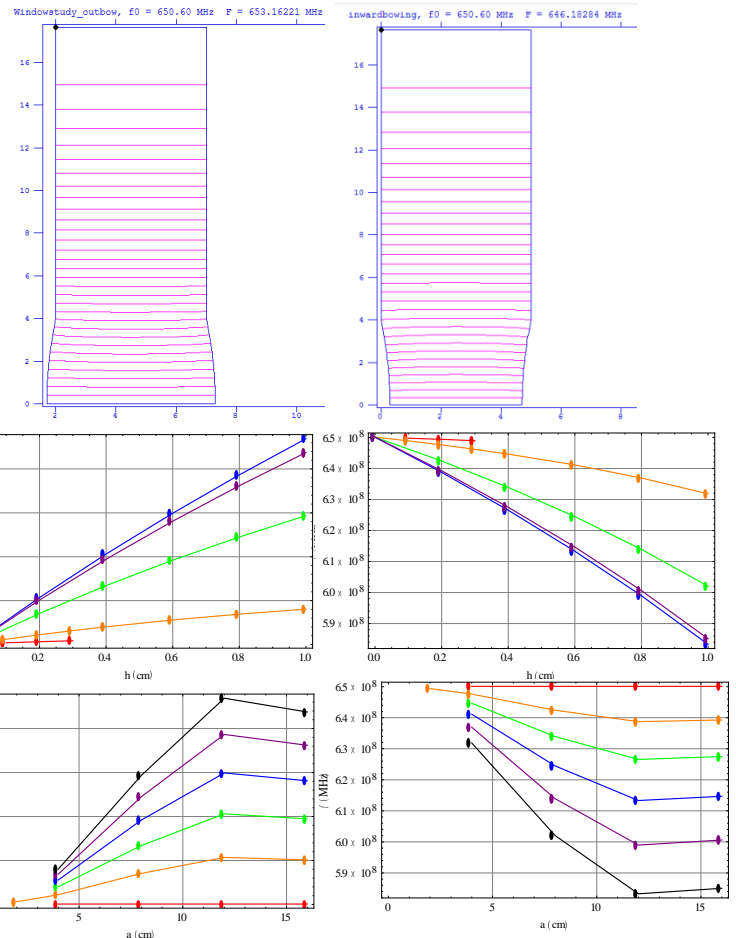


Figure 7: Images of SF outputs (top), plot of change in frequency vs. bow height (middle) and change in frequency vs. window radius (bottom). In the middle plots (outbow left, inbow right) the colors correspond to window radii of 2cm (red), 4cm (green), 8cm (blue), and 12cm (orange). In the bottom plots (inbow right, outbow left) the colors correspond to bow heights of 0.0cm (red), 0.2cm (orange), 0.4cm (green), 0.6cm (blue), 0.8cm (purple), and 1.0cm (black).

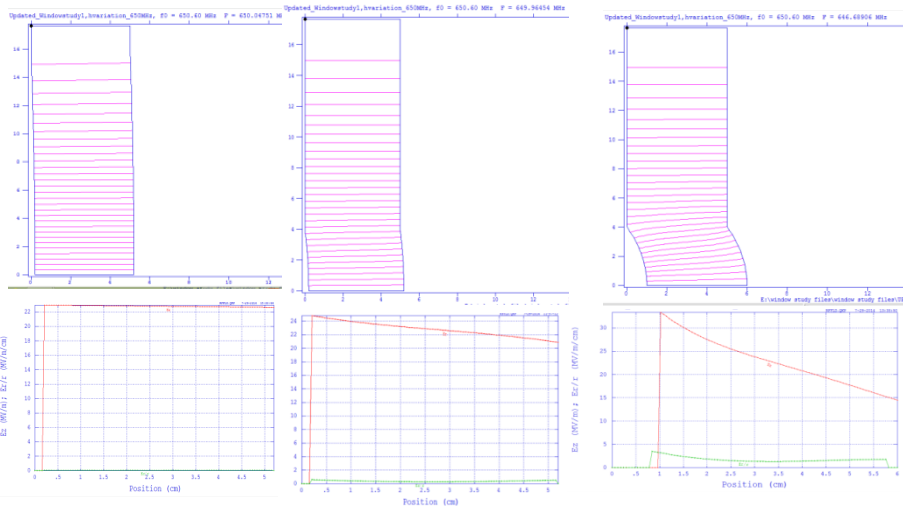


Figure 8: SF outputs (top) of cavities with length 5 cm, window radii of 16 (left) and 4 (middle and right). The bottom Parmela outputs correspond to the SF outputs above them.

The electric field inside cavities with outward bowing windows (figure 9, top) increased from the first window to the middle of the cavity but decreased back to the starting value at the second window. The electric field for cavities with inward bowing windows (figure 9, bottom) decreased from the first window towards the middle of the cavity, then increased from the middle to the second window. In the both of the cases of inward bowing windows

and outward bowing windows, there is no net change in the electric field between the two windows. This implies that there is no net acceleration of charged particles in these cavities.

### Future Work

The results discussed here are only a fraction of the studies that will be done to ensure the most effective and efficient RF cavity design for a Muon channel. Currently, there are several more tests being conducted on cavity window bowing and theoretical modeling. Bowed window simulations are being run under similar conditions as the one presented in this paper. There will be more investigation into a theoretical model to explain the phenomenon observed in the structures discussed here to ensure the best possible fit. This will require finer steps in simulation runs, such as changing bow height in increments of 0.1 cm instead of 0.2.

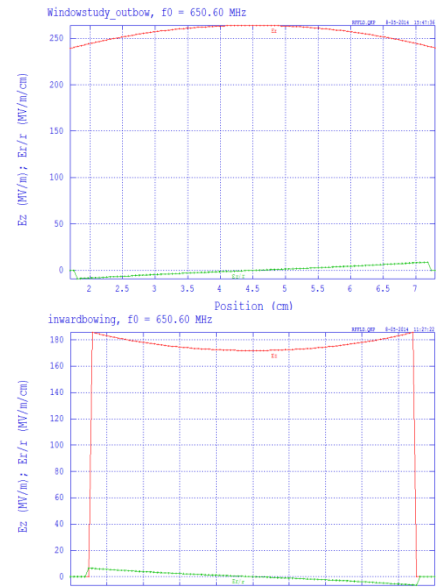


Figure 9: Parmela outputs for cavities with an inward bow (bottom) and outward bow (top).

### Acknowledgements

This project was made possible by Fermilab and the Department Of Energy (DOE), the SIST program and program committee, and supervisor Katsuya Yonehara of the RF technology group. I would like to give a special thanks to Ben Freemire, Alvin Tollestrope, and Albert Moretti for their support, teachings, and patience.

## References

- [1] K. Yonehara, International Particle Accelerator Conference, 2012.
- [2] L.m.Nash, et al., IPAC 2013, pp. 1508.
- [3] Los Alamos National Laboratory, University of California, Last modified and Fri 06 Jul 2012, accessed 8/7/2014.